



## Original Article

## Radiation protective qualities of some selected lead and bismuth salts in the wide gamma energy region

M.I. Sayyed <sup>a</sup>, F. Akman <sup>b,\*</sup>, M.R. Kaçal <sup>c</sup>, A. Kumar <sup>d</sup><sup>a</sup> University of Tabuk, Faculty of Science, Department of Physics, Tabuk, KSA, Saudi Arabia<sup>b</sup> Bingöl University, Vocational School of Technical Sciences, Department of Electronic Communication Technology, 12000, Bingöl, Turkey<sup>c</sup> Giresun University, Arts and Sciences Faculty, Department of Physics, 28100, Giresun, Turkey<sup>d</sup> Department of Physics, University College, Benra-Dhuri, Punjab, India

## ARTICLE INFO

## Article history:

Received 11 September 2018

Received in revised form

19 December 2018

Accepted 21 December 2018

Available online 23 December 2018

## Keywords:

Lead

Bismuth

Photon

HPGe detector

Radiation protection efficiency

## ABSTRACT

The lead element or its salts are good radiation shielding materials. However, their toxic effects are high. Due to less toxicity of bismuth salts, the radiation shielding properties of the bismuth salts have been investigated and compared to that of lead salts to establish them as a better alternative to radiation shielding material to the lead element or its salts. The transmission geometry was utilized to measure the mass attenuation coefficient ( $\mu/\rho$ ) of different salts containing lead and bismuth using a high-resolution HPGe detector and different energies (between 81 and 1333 keV) emitted from point sources of  $^{133}\text{Ba}$ ,  $^{57}\text{Co}$ ,  $^{22}\text{Na}$ ,  $^{54}\text{Mn}$ ,  $^{137}\text{Cs}$ , and  $^{60}\text{Co}$ . The experimental  $\mu/\rho$  results are compared with the theoretical values obtained through WinXCOM program. The theoretical calculations are in good agreement with their experimental ones. The radiation protection efficiencies, mean free paths, effective atomic numbers and electron densities for the present compounds were determined. The bismuth fluoride ( $\text{BiF}_3$ ) is found to have maximum radiation protection efficiency among the selected salts. The results showed that present salts are more effective for reducing the intensity of gamma photons at low energy region.

© 2018 Korean Nuclear Society, Published by Elsevier Korea LLC. This is an open access article under the CC BY-NC-ND license (<http://creativecommons.org/licenses/by-nc-nd/4.0/>).

## 1. Introduction

The contributions of nuclear power and nuclear technology in different areas of everyday life like the production of electricity by nuclear power stations, the world of dentistry and medicine via dental imaging and radiotherapy, food irradiation, inspection and instrumentation, desalination, sterilization, and industry have been significantly improved.

Although nuclear technology has different applications in our life, it also has several disadvantages. One of the major disadvantages of the nuclear technology is the contamination caused by the radiation to the environment and to a massive area of surrounding land. Therefore, it is important to reduce the leakage of the radiation by using some materials that can attenuate the radiation, which is known as shielding materials [1–5]. In this regard, different investigators developed several types of concrete which possess excellent radiation attenuation parameters [6–8]. In addition, recently some researchers try to prepare different glass

systems that can be used as radiation shielding materials [9–12]. Besides, several investigators have developed polymer composites for the radiation shielding purposes [13–15].

Lead ( $\text{Pb}$ ,  $Z = 82$ ) and its derivatives are the most common radiation shielding materials since they have high value of the mass attenuation coefficient for gamma radiations and provide best shield against gamma radiations. Also, they have other applications in various fields such as lead salt have been widely utilized as sensors for infrared (IR) radiation, optoelectronic devices, solar cells and photo-resistors [16]. However, recently, due to the toxicity of the lead, the investigators are now focused on developing alternatives to the lead and its derivative that can be employed for high-energy radiations such as gamma radiation.

In this context, bismuth ( $\text{Bi}$ ,  $Z = 83$ ) is one of the less toxic heavy metals. The bismuth compounds are attractive for use in different applications. For example, they used as catalysts, in addition to the pharmaceuticals industry via the substitution of toxic  $\text{Pb}$  to the electronics industry [17]. Also, recently bismuth oxide ( $\text{Bi}_2\text{O}_3$ ) is used in the preparation of different glass systems that used for radiation shielding.

Accurate values of some quantities such as mass attenuation coefficient ( $\mu/\rho$ ), effective atomic number ( $Z_{\text{eff}}$ ), and mean free path,

\* Corresponding author.

E-mail address: [fakman@bingol.edu.tr](mailto:fakman@bingol.edu.tr) (F. Akman).

**Table 1**

The chemical formula and density of the selected samples.

Sample Name	Chemical Formula	Density (g/cm <sup>3</sup> )
Bismuth (III) chloride oxide	BiClO	7.72
Bismuth (III) bromide	BiBr <sub>3</sub>	5.70
Bismuth (III) fluoride	BiF <sub>3</sub>	5.32
Bismuth (III) iodide	BiI <sub>3</sub>	5.78
Lead (II) sulfate	PbSO <sub>4</sub>	6.29
Lead (II) chloride	PbCl <sub>2</sub>	5.85
Lead (II) bromide	PbBr <sub>2</sub>	6.66
Lead (II) iodide	PbI <sub>2</sub>	6.16

which estimate the absorption and scattering of gamma radiation with matter, are important to judge a material's practical application in radiation protection. Frequently, photon interaction is dependent on many factors like the energy of the photon, the density of the material, and the atomic number of elements present in the materials [18–20].

The main aim of the current work is to investigate the photon attenuation parameters of different lead and bismuth salts. The mass attenuation coefficients ( $\mu/\rho$ ) for the selected lead and bismuth salts have been measured experimentally using the transmission geometry in the energy range of 81 keV–1333 keV. Besides, the  $\mu/\rho$  values have been calculated theoretically using WinXCOM program [21]. Furthermore, the radiation protection efficiencies, mean free paths, effective atomic number and electron densities of the present samples were determined.

## 2. Materials and method

In the present work, the transmission geometry was utilized to measure the  $\mu/\rho$  of the following compounds containing lead and bismuth: bismuth chloride oxide, bismuth bromide, bismuth fluoride, bismuth iodide, lead sulfate, lead chloride, lead bromide and lead iodide. The various Pb and Bi salts have been purchased from Sigma-Aldrich Company. Each sample was prepared with the help of hydraulic press by applying 15-ton press per cm<sup>2</sup>. The samples were disc shaped having 13 mm diameter and different masses. The mass per unit area values were determined as 0.504–1.067 g/cm<sup>2</sup> for Bi salts and 0.410–0.748 g/cm<sup>2</sup> for Pb salts. The chemical formula and the density of the selected samples are listed in Table 1.

The experimental setup used in the experiments is given in Fig. 1. In the experiments, 81, 161, 276, 303, 356 and 384 keV from <sup>133</sup>Ba, 122 and 136 keV from <sup>57</sup>Co, 511 and 1275 keV from <sup>22</sup>Na, 835 keV from <sup>54</sup>Mn, 662 keV from <sup>137</sup>Cs, 1173 and 1333 keV from <sup>60</sup>Co photon energies were used. Besides, an HPGe detector (Ortec trademark, GEM-SP7025P4-B model) with an active crystal diameter of 70 mm and an active crystal length of 25 mm, with a resolution of 380 eV at 5.9 keV, 585 eV at 122 keV and 1.8 keV at 1.33 MeV was used in the experiments. The experimental measurements were repeated three times to determine the selected parameters. For sufficient statistical accuracy, the spectrum of each source (with and without absorber) was recorded for 1000 s. The detailed experimental procedure can be found in our recent paper [22]. The radiation protection efficiency results were determined using the initial and transmitted gamma intensities (i.e.  $I_0$  and  $I$ ). The mean free path, effective atomic number and electron density results were calculated with the help of the obtained mass attenuation coefficients.

## 3. Results and discussion

The values of linear attenuation coefficient ( $\mu$ ) have been measured at several photon energies from the measured incident and transmitted photon intensities ( $I_0$  and  $I$ ) for the samples in a narrow beam geometrical setup. The experimental values of  $\mu/\rho$  have also been obtained from the above measured values by dividing with the densities of the respective compounds. These values are enlisted in Table 2 together with the estimated uncertainty in experimental measurements obtained with the following formula:

$$\Delta\left(\frac{\mu}{\rho}\right) = \frac{1}{\rho x} \sqrt{\left(\frac{\Delta I_0}{I_0}\right)^2 + \left(\frac{\Delta I}{I}\right)^2 + \left(\ln \frac{I_0}{I}\right)^2 \cdot \left(\frac{\Delta \rho x}{\rho x}\right)^2} \quad (1)$$

where,  $\Delta I_0$  and  $\Delta I$  are the uncertainties in the measurement of  $I_0$  and  $I$ , respectively and  $\Delta \rho x$  is the uncertainty in the measurement of mass per unit area of the sample. These uncertainties are due to the uncertainties in the measurements of the areas under the related  $\gamma$ -ray peaks, mass per unit area of the samples and statistical uncertainties in the measurements of incident ( $I$ ) and transmitted ( $I_0$ ) intensities. The maximum uncertainties are 4.39% in BiClO, 4.76% in BiBr<sub>3</sub>, 4.96% in BiF<sub>3</sub>, 4.64% in BiI<sub>3</sub>, 4.45% in PbSO<sub>4</sub>, 3.84% in PbCl<sub>2</sub>, 3.95% in PbBr<sub>2</sub> and 3.96% in PbI<sub>2</sub>, respectively. The

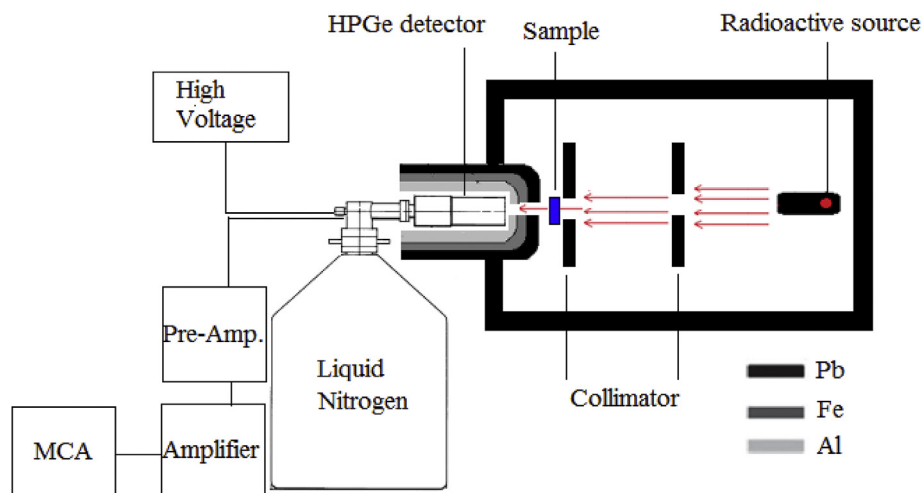


Fig. 1. The experimental setup.

**Table 2**The mass attenuation coefficients ( $\text{cm}^2/\text{g}$ ) of the selected samples.

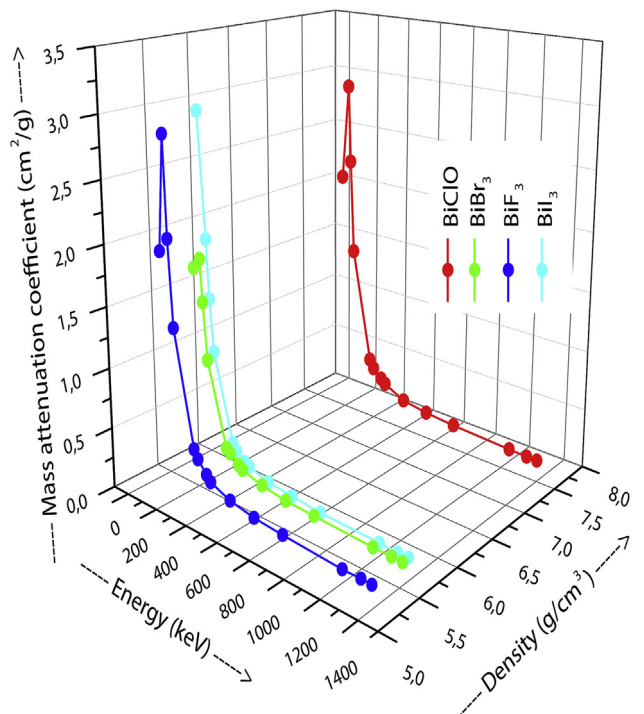
Energy (keV)	BiClO		BiBr <sub>3</sub>		BiF <sub>3</sub>		BiI <sub>3</sub>	
	Exp.	WinX.	Exp.	WinX.	Exp.	WinX.	Exp.	WinX.
81	2.0603 ± 0.0238	2.0080	1.7124 ± 0.0197	1.7585	1.9382 ± 0.0289	1.9557	2.9529 ± 0.0416	3.0586
122	2.8884 ± 0.0825	2.8206	1.8014 ± 0.0363	1.8514	2.8567 ± 0.0487	2.7601	1.9423 ± 0.0473	1.9799
136	2.2191 ± 0.0973	2.1416	1.4483 ± 0.0689	1.4108	2.0563 ± 0.1020	2.0963	1.4533 ± 0.0675	1.4988
161	1.3966 ± 0.0550	1.4393	0.9764 ± 0.0256	0.9567	1.3550 ± 0.0672	1.4095	1.0217 ± 0.0303	1.0070
276	0.4110 ± 0.0160	0.4190	0.2933 ± 0.0110	0.2988	0.4222 ± 0.0185	0.4115	0.3039 ± 0.0116	0.3054
303	0.3382 ± 0.0080	0.3484	0.2623 ± 0.0061	0.2530	0.3561 ± 0.0092	0.3424	0.2492 ± 0.0058	0.2574
356	0.2669 ± 0.0031	0.2572	0.1977 ± 0.0023	0.1934	0.2611 ± 0.0031	0.2531	0.1890 ± 0.0022	0.1953
384	0.2312 ± 0.0070	0.2255	0.1703 ± 0.0049	0.1724	0.2156 ± 0.0066	0.2220	0.1703 ± 0.0050	0.1736
511	0.1418 ± 0.0017	0.1453	0.1158 ± 0.0014	0.1186	0.1455 ± 0.0018	0.1435	0.1138 ± 0.0014	0.1182
662	0.1064 ± 0.0013	0.1052	0.0879 ± 0.0011	0.0905	0.1043 ± 0.0013	0.1042	0.0916 ± 0.0011	0.0897
835	0.0835 ± 0.0023	0.0827	0.0773 ± 0.0022	0.0739	0.0850 ± 0.0025	0.0820	0.0703 ± 0.0020	0.0730
1173	0.0617 ± 0.0008	0.0615	0.0565 ± 0.0007	0.0573	0.0589 ± 0.0007	0.0611	0.0573 ± 0.0007	0.0564
1275	0.0563 ± 0.0006	0.0579	0.0565 ± 0.0007	0.0543	0.0595 ± 0.0007	0.0575	0.0510 ± 0.0006	0.0534
1333	0.0577 ± 0.0006	0.0562	0.0552 ± 0.0006	0.0528	0.0580 ± 0.0007	0.0559	0.0542 ± 0.0006	0.0520
Energy (keV)	PbSO <sub>4</sub>		PbCl <sub>2</sub>		PbBr <sub>2</sub>		PbI <sub>2</sub>	
	Exp.	WinX.	Exp.	WinX.	Exp.	WinX.	Exp.	WinX.
81	1.5890 ± 0.0177	1.6647	1.7712 ± 0.0200	1.8151	1.7748 ± 0.0218	1.8295	2.8117 ± 0.0353	2.9237
122	2.3105 ± 0.0472	2.3439	2.4259 ± 0.0509	2.5463	2.0026 ± 0.0597	2.0863	2.1340 ± 0.0486	2.1480
136	1.7600 ± 0.0783	1.7853	1.8535 ± 0.0711	1.9363	1.5493 ± 0.0612	1.5878	1.5656 ± 0.0620	1.6268
161	1.1660 ± 0.0359	1.2062	1.2502 ± 0.0330	1.3042	1.0852 ± 0.0346	1.0727	1.1289 ± 0.0362	1.0919
276	0.3489 ± 0.0133	0.3626	0.3914 ± 0.0145	0.3848	0.3149 ± 0.0122	0.3260	0.3111 ± 0.0118	0.3262
303	0.2961 ± 0.0070	0.3041	0.3133 ± 0.0076	0.3213	0.2828 ± 0.0067	0.2744	0.2820 ± 0.0067	0.2738
356	0.2304 ± 0.0027	0.2282	0.2343 ± 0.0027	0.2390	0.2147 ± 0.0025	0.2074	0.2047 ± 0.0024	0.2061
384	0.2103 ± 0.0063	0.2017	0.2090 ± 0.0062	0.2104	0.1792 ± 0.0053	0.1839	0.1774 ± 0.0054	0.1826
511	0.1310 ± 0.0016	0.1342	0.1406 ± 0.0017	0.1377	0.1211 ± 0.0015	0.1240	0.1185 ± 0.0014	0.1226
662	0.0961 ± 0.0012	0.0998	0.0988 ± 0.0012	0.1011	0.0898 ± 0.0011	0.0932	0.0896 ± 0.0011	0.0920
835	0.0818 ± 0.0022	0.0800	0.0769 ± 0.0022	0.0802	0.0779 ± 0.0023	0.0753	0.0769 ± 0.0021	0.0742
1173	0.0592 ± 0.0007	0.0608	0.0626 ± 0.0008	0.0604	0.0575 ± 0.0007	0.0578	0.0552 ± 0.0007	0.0569
1275	0.0563 ± 0.0006	0.0574	0.0586 ± 0.0007	0.0570	0.0526 ± 0.0006	0.0546	0.0554 ± 0.0006	0.0538
1333	0.0540 ± 0.0006	0.0558	0.0560 ± 0.0006	0.0553	0.0539 ± 0.0006	0.0532	0.0507 ± 0.0006	0.0524

measured  $\mu/\rho$  values are also compared with the theoretical values of mass attenuation coefficients obtained through WinXCOM, and are represented in Table 2. The maximum difference between the experimental and theoretical values of  $\mu/\rho$  is 3.79% in BiClO, 4.63% in BiBr<sub>3</sub>, 4.00% in BiF<sub>3</sub>, 4.52% in BiI<sub>3</sub>, 4.55% in PbSO<sub>4</sub>, 4.73% in PbCl<sub>2</sub>, 4.01% in PbBr<sub>2</sub> and 4.61% in PbI<sub>2</sub>, respectively. Hence, we can conclude that the experimental findings are in good agreement with their theoretical ones. The variation of mass attenuation coefficients as a function of energy is represented in Fig. 2 and Fig. 3, respectively for the compounds containing Bi and Pb, respectively. The  $\mu/\rho$  values increases to maximum at 122 keV and thereafter decreases exponentially with increasing energy. It is due to the dominance of the photoelectric and Compton radiation interaction process respectively in different energy regions. Similar results were also obtained by Obaid et al. [23] and Gaikwad et al. [24].

The radiation protection efficiency (RPE) is a very important parameter to establish the effectiveness of a shielding material. The initial and transmitted intensities (i.e  $I_0$  and  $I$ ) are related to the radiation protection efficiency (RPE) through equation (2) [25]:

$$RPE = \left( 1 - \frac{I}{I_0} \right) \times 100 \quad (2)$$

The radiation protection efficiencies for the selected compounds are obtained and summarized in Table 3. The BiF<sub>3</sub> was found to have maximum RPE among the compounds under study. It indicates the better shielding performance of Bismuth fluoride (BiF<sub>3</sub>). Also, from Table 3 it is clear that more gamma photons being transmitted as the energy increases. On the other words, the present compounds are more effective for reducing the intensity of gamma photons at

**Fig. 2.** Variation of mass attenuation coefficients with energy of samples containing Bi.

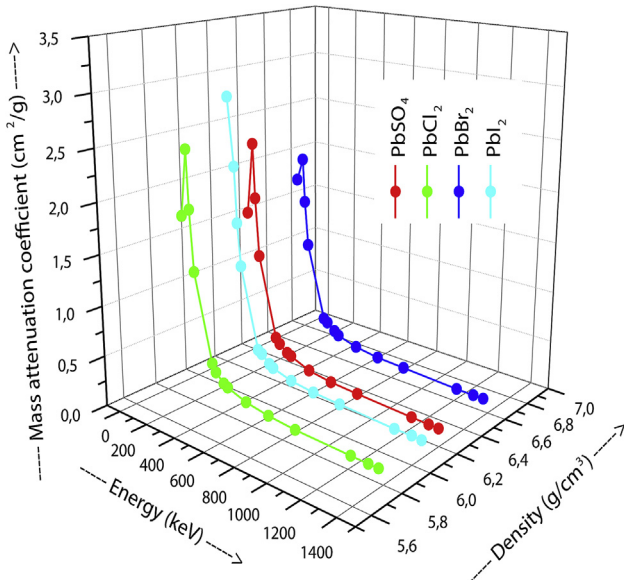


**Fig. 3.** Variation of mass attenuation coefficients with energy of samples containing Pb.

low energy. Therefore, to improve the shielding properties for the compounds under study we must increase the thickness of the sample.

The mean free path (MFP) is another parameter to compare the shielding competence of a material. If the material has a lower mean free path, it is a better shielding material [26]. The MFP is the reciprocal of  $\mu$ . The experimentally measured and the theoretical values of MFP are represented in Table 4 and are found to be in good agreement. The variation of the MFP as a function of energy is represented in Fig. 4 and Fig. 5, respectively for the compounds containing Bi and Pb. Based on the MFP,  $\text{BiClO}$  has the lowest MFP values thus has a good shielding performance. In general, the MFP value of any sample decreases with increasing the density, and according to Table 1,  $\text{BiClO}$  has the highest density so it is expected to possess low MFP. It is found that the mean free path is low at low energies and is increasing at higher energies. Thus, the selected compounds have good shielding properties at low energies and their shielding competence decreases with energy. Generally, Figs. 4 and 5 show that the MFP increases versus the photon energy for all the compounds containing Bi and Pb. This means that more

photons can penetrate the present compounds as the energy increases, and the compounds under study can attenuate more gamma radiation at low photon energy.

The other parameters are the effective atomic number and effective electron density. The large values of effective atomic number and electron density are indicative of good radiation shielding properties of the material. Since the selected compounds containing Bi and Pb are composed of more than one element, it is useful to characterize the properties of the compounds in terms of equivalent elements, which is known as the effective atomic number ( $Z_{\text{eff}}$ ) [27]. The details of the  $Z_{\text{eff}}$  calculations are available elsewhere [28,29]. The  $Z_{\text{eff}}$  values are determined experimentally, and the experimental  $Z_{\text{eff}}$  values along with the theoretical ones are represented in Table 5 and it is observed that they are in good agreement. The values of  $Z_{\text{eff}}$  range from 40.231 to 78.176 for  $\text{BiClO}$ , 49.291 to 70.787 for  $\text{BiBr}_3$ , 31.347 to 76.224 for  $\text{BiF}_3$ , 61.630 to 68.371 for  $\text{BiI}_3$ , 24.414 to 71.118 for  $\text{PbSO}_4$ , 42.397 to 76.964 for  $\text{PbCl}_2$ , 53.168 to 73.072 for  $\text{PbBr}_2$  and 63.877 to 70.533 for  $\text{PbI}_2$ , respectively. It is clearly seen from Table 5 that  $Z_{\text{eff}}$  increases to maximum at 122 keV and thereafter decreases with increasing energy. It is obvious that the  $Z_{\text{eff}}$  values for all compounds are high for the photon with low energy. The photoelectric interaction (PE) normally dominates in the lower gamma radiation energy values and for the high atomic number of the absorbing materials. The probability for the PE (known as the cross section) to occur is dependent upon  $Z^{4-5}/E^{3.5}$  [30].

The  $Z_{\text{eff}}$  is related to another parameter known as the effective electron density ( $N_e$ ), which represents the number of electrons per unit mass of the interacting materials [31]. The determined experimental and theoretical values of electron density are represented in Table 6 and they are in good agreement. The values of  $N_e$  range from  $(2.791-5.423) \times 10^{23}$  for  $\text{BiClO}$ ,  $(4.110-5.903) \times 10^{23}$  for  $\text{BiBr}_3$ ,  $(3.312-8.054) \times 10^{23}$  for  $\text{BiF}_3$ ,  $(4.420-4.904) \times 10^{23}$  for  $\text{BiI}_3$ ,  $(3.456-10.067) \times 10^{23}$  for  $\text{PbSO}_4$ ,  $(3.157-5.730) \times 10^{23}$  for  $\text{PbCl}_2$ ,  $(3.346-4.598) \times 10^{23}$  for  $\text{PbBr}_2$ ,  $(3.454-3.814) \times 10^{23}$  for  $\text{PbI}_2$ , respectively. Table 6 revealed that the dependence of the  $N_e$  of the compounds containing Bi and Pb versus the energy is similar to that obtained for  $Z_{\text{eff}}$ . This trend was also observed for several materials such as rocks [5], biological compounds [24], amino acids [32], plants [33], soils [34] and triazoles samples [35].

#### 4. Conclusion

In the carried out study, the mass attenuation coefficients, radiation protection efficiencies, mean free paths, effective atomic

**Table 3**

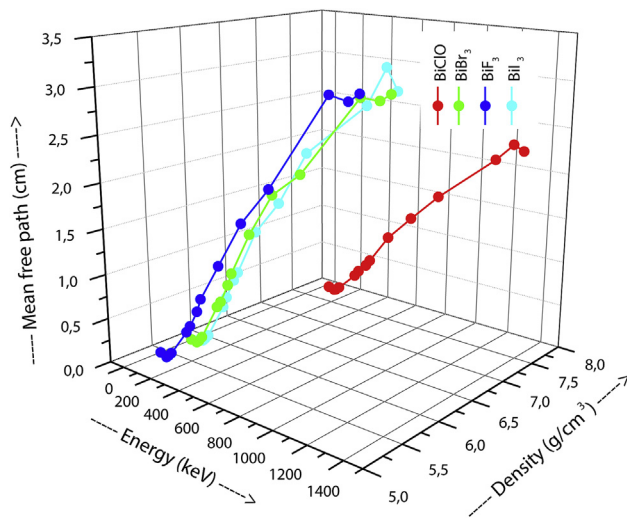
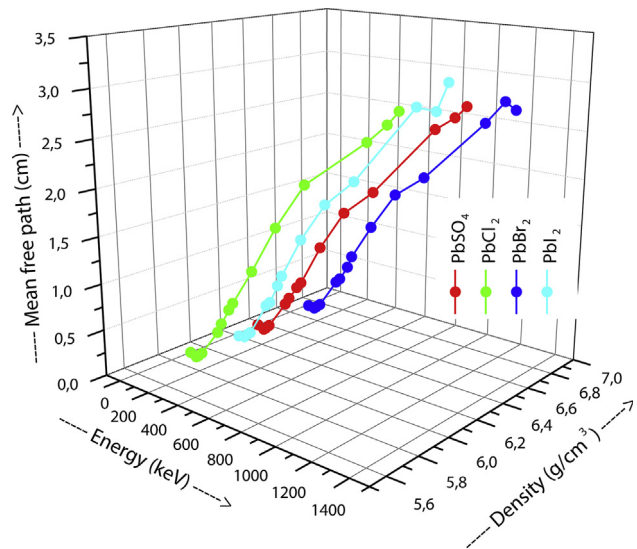
The radiation protection efficiencies of the selected samples.

Energy (keV)	$\text{BiClO}$	$\text{BiBr}_3$	$\text{BiF}_3$	$\text{BiI}_3$	$\text{PbSO}_4$	$\text{PbCl}_2$	$\text{PbBr}_2$	$\text{PbI}_2$
81	$64.62 \pm 0.37$	$58.79 \pm 0.33$	$87.35 \pm 0.97$	$84.53 \pm 0.84$	$47.88 \pm 0.24$	$51.95 \pm 0.27$	$73.57 \pm 0.53$	$76.97 \pm 0.58$
122	$76.70 \pm 2.05$	$60.65 \pm 1.06$	$95.25 \pm 1.32$	$70.71 \pm 1.57$	$61.23 \pm 1.09$	$63.36 \pm 1.17$	$77.72 \pm 2.18$	$67.19 \pm 1.37$
136	$67.34 \pm 2.88$	$52.75 \pm 2.45$	$88.85 \pm 4.31$	$60.09 \pm 2.72$	$51.41 \pm 2.23$	$53.56 \pm 1.98$	$68.70 \pm 2.62$	$55.85 \pm 2.14$
161	$50.55 \pm 1.92$	$39.68 \pm 0.96$	$76.44 \pm 3.71$	$47.58 \pm 1.33$	$38.00 \pm 1.11$	$40.39 \pm 0.99$	$55.68 \pm 1.69$	$44.54 \pm 1.36$
276	$18.72 \pm 0.70$	$14.09 \pm 0.51$	$36.27 \pm 1.55$	$17.48 \pm 0.64$	$13.33 \pm 0.49$	$14.95 \pm 0.53$	$21.03 \pm 0.78$	$15.00 \pm 0.55$
303	$15.68 \pm 0.34$	$12.70 \pm 0.27$	$31.61 \pm 0.75$	$14.58 \pm 0.31$	$11.43 \pm 0.24$	$12.16 \pm 0.27$	$19.11 \pm 0.41$	$13.69 \pm 0.30$
356	$12.59 \pm 0.07$	$9.73 \pm 0.06$	$24.31 \pm 0.16$	$11.26 \pm 0.07$	$9.01 \pm 0.05$	$9.24 \pm 0.05$	$14.87 \pm 0.09$	$10.14 \pm 0.06$
384	$11.00 \pm 0.31$	$8.44 \pm 0.23$	$20.55 \pm 0.60$	$10.20 \pm 0.28$	$8.26 \pm 0.23$	$8.29 \pm 0.23$	$12.57 \pm 0.35$	$8.85 \pm 0.25$
511	$6.90 \pm 0.05$	$5.82 \pm 0.04$	$14.38 \pm 0.10$	$6.94 \pm 0.05$	$5.23 \pm 0.03$	$5.65 \pm 0.04$	$8.68 \pm 0.06$	$6.00 \pm 0.04$
662	$5.22 \pm 0.04$	$4.45 \pm 0.03$	$10.53 \pm 0.07$	$5.63 \pm 0.04$	$3.86 \pm 0.03$	$4.00 \pm 0.03$	$6.51 \pm 0.04$	$4.57 \pm 0.03$
835	$4.13 \pm 0.10$	$3.92 \pm 0.10$	$8.67 \pm 0.24$	$4.35 \pm 0.12$	$3.30 \pm 0.08$	$3.13 \pm 0.08$	$5.68 \pm 0.15$	$3.93 \pm 0.10$
1173	$3.06 \pm 0.02$	$2.88 \pm 0.02$	$6.09 \pm 0.04$	$3.56 \pm 0.03$	$2.40 \pm 0.02$	$2.56 \pm 0.02$	$4.22 \pm 0.03$	$2.84 \pm 0.02$
1275	$2.80 \pm 0.02$	$2.88 \pm 0.02$	$6.15 \pm 0.04$	$3.17 \pm 0.02$	$2.28 \pm 0.01$	$2.40 \pm 0.01$	$3.86 \pm 0.02$	$2.85 \pm 0.02$
1333	$2.87 \pm 0.01$	$2.82 \pm 0.01$	$6.00 \pm 0.03$	$3.37 \pm 0.02$	$2.19 \pm 0.01$	$2.29 \pm 0.01$	$3.96 \pm 0.02$	$2.61 \pm 0.01$

**Table 4**

The mean free path (cm) of the selected samples.

Energy (keV)	BiClO		BiBr <sub>3</sub>		BiF <sub>3</sub>		BiI <sub>3</sub>	
	Exp.	Theo.	Exp.	Theo.	Exp.	Theo.	Exp.	Theo.
81	0.0629 ± 0.0007	0.0645	0.1025 ± 0.0012	0.0998	0.0970 ± 0.0014	0.0961	0.0586 ± 0.0008	0.0566
122	0.0448 ± 0.0013	0.0459	0.0974 ± 0.0020	0.0948	0.0658 ± 0.0011	0.0681	0.0891 ± 0.0022	0.0874
136	0.0584 ± 0.0026	0.0605	0.1211 ± 0.0058	0.1244	0.0914 ± 0.0045	0.0897	0.1190 ± 0.0055	0.1154
161	0.0927 ± 0.0036	0.0900	0.1797 ± 0.0047	0.1834	0.1387 ± 0.0069	0.1334	0.1693 ± 0.0050	0.1718
276	0.3151 ± 0.0123	0.3092	0.5981 ± 0.0224	0.5872	0.4452 ± 0.0195	0.4568	0.5694 ± 0.0218	0.5664
303	0.3830 ± 0.0091	0.3718	0.6689 ± 0.0155	0.6935	0.5278 ± 0.0136	0.5490	0.6942 ± 0.0161	0.6721
356	0.4853 ± 0.0056	0.5037	0.8873 ± 0.0103	0.9073	0.7199 ± 0.0086	0.7426	0.9152 ± 0.0107	0.8860
384	0.5603 ± 0.0170	0.5745	1.0302 ± 0.0296	1.0175	0.8717 ± 0.0268	0.8466	1.0160 ± 0.0297	0.9967
511	0.9133 ± 0.0109	0.8916	1.5150 ± 0.0180	1.4798	1.2919 ± 0.0157	1.3103	1.5205 ± 0.0182	1.4638
662	1.2176 ± 0.0148	1.2308	1.9964 ± 0.0240	1.9383	1.8019 ± 0.0219	1.8047	1.8887 ± 0.0228	1.9291
835	1.5506 ± 0.0421	1.5670	2.2696 ± 0.0647	2.3746	2.2120 ± 0.0646	2.2936	2.4619 ± 0.0714	2.3709
1173	2.1007 ± 0.0258	2.1048	3.1057 ± 0.0380	3.0631	3.1929 ± 0.0392	3.0749	3.0180 ± 0.0371	3.0693
1275	2.3027 ± 0.0265	2.2363	3.1043 ± 0.0357	3.2332	3.1602 ± 0.0364	3.2663	3.3919 ± 0.0391	3.2386
1333	2.2462 ± 0.0252	2.3040	3.1778 ± 0.0356	3.3218	3.2414 ± 0.0365	3.3649	3.1915 ± 0.0357	3.3268
Energy (keV)	PbSO <sub>4</sub>		PbCl <sub>2</sub>		PbBr <sub>2</sub>		PbI <sub>2</sub>	
	Exp.	Theo.	Exp.	Theo.	Exp.	Theo.	Exp.	Theo.
81	0.1001 ± 0.0011	0.0955	0.0965 ± 0.0011	0.0942	0.0846 ± 0.0010	0.0821	0.0577 ± 0.0007	0.0555
122	0.0688 ± 0.0014	0.0678	0.0705 ± 0.0015	0.0671	0.0750 ± 0.0022	0.0720	0.0761 ± 0.0017	0.0756
136	0.0903 ± 0.0040	0.0890	0.0922 ± 0.0035	0.0883	0.0969 ± 0.0038	0.0946	0.1037 ± 0.0041	0.0998
161	0.1364 ± 0.0042	0.1318	0.1367 ± 0.0036	0.1311	0.1384 ± 0.0044	0.1400	0.1438 ± 0.0046	0.1487
276	0.4557 ± 0.0174	0.4385	0.4367 ± 0.0162	0.4442	0.4769 ± 0.0184	0.4605	0.5218 ± 0.0198	0.4977
303	0.5369 ± 0.0126	0.5229	0.5457 ± 0.0132	0.5321	0.5309 ± 0.0126	0.5472	0.5757 ± 0.0137	0.5929
356	0.6901 ± 0.0080	0.6967	0.7297 ± 0.0085	0.7152	0.6992 ± 0.0082	0.7241	0.7931 ± 0.0092	0.7875
384	0.7561 ± 0.0226	0.7883	0.8178 ± 0.0244	0.8126	0.8380 ± 0.0246	0.8164	0.9149 ± 0.0278	0.8893
511	1.2134 ± 0.0144	1.1850	1.2157 ± 0.0146	1.2413	1.2397 ± 0.0148	1.2111	1.3698 ± 0.0164	1.3245
662	1.6550 ± 0.0200	1.5932	1.7307 ± 0.0209	1.6907	1.6717 ± 0.0202	1.6103	1.8110 ± 0.0219	1.7649
835	1.9427 ± 0.0525	1.9885	2.2241 ± 0.0625	2.1307	1.9266 ± 0.0556	1.9938	2.1118 ± 0.0588	2.1866
1173	2.6843 ± 0.0329	2.6135	2.7328 ± 0.0334	2.8287	2.6127 ± 0.0320	2.5984	2.9409 ± 0.0357	2.8527
1275	2.8240 ± 0.0325	2.7685	2.9152 ± 0.0335	3.0008	2.8570 ± 0.0328	2.7478	2.9277 ± 0.0335	3.0147
1333	2.9446 ± 0.0329	2.8486	3.0511 ± 0.0341	3.0891	2.7869 ± 0.0312	2.8248	3.2048 ± 0.0359	3.0984

**Fig. 4.** Variation of mean free path with energy of samples containing Bi.**Fig. 5.** Variation of mean free path with energy of samples containing Pb.

numbers and electron densities were obtained for some selected Pb and Bi salts in the energy range of 81 keV–1333 keV with the aid of the transmission geometry including a high-resolution HPGe detector and six different radioactive point sources. It is generally observed that there is a good agreement between experimental and theoretical data. The following conclusions were reached; the highest mass attenuation coefficients, radiation protection efficiencies, effective atomic numbers and electron densities have BiI<sub>3</sub>, BiF<sub>3</sub>, BiClO and PbSO<sub>4</sub> salts, respectively. In addition, the lowest

mean free paths have BiClO salt among the selected salts. According to these results, the above-mentioned radiation shielding parameters depend on the atomic number, weight fraction, and atomic weight of elements in the material and the density of material. The obtained results are undoubtedly very important for radiation physics, health physics, radiation shielding and space studies.

**Table 5**

The effective atomic number of the selected samples.

Energy (keV)	BiClO		BiBr <sub>3</sub>		BiF <sub>3</sub>		Bil <sub>3</sub>	
	Exp.	Theo.	Exp.	Theo.	Exp.	Theo.	Exp.	Theo.
81	76.199 ± 0.881	74.263	54.483 ± 0.627	55.951	71.723 ± 1.069	72.371	57.004 ± 0.803	59.045
122	80.056 ± 2.285	78.176	68.876 ± 1.386	70.787	78.892 ± 1.345	76.224	67.073 ± 1.632	68.371
136	79.885 ± 3.504	77.096	72.207 ± 3.434	70.337	73.176 ± 3.628	74.596	66.299 ± 3.078	68.377
161	72.858 ± 2.867	75.083	70.772 ± 1.858	69.350	68.870 ± 3.416	71.643	69.277 ± 2.055	68.280
276	63.159 ± 2.457	64.376	62.063 ± 2.324	63.221	58.811 ± 2.579	57.313	66.544 ± 2.543	66.890
303	60.332 ± 1.433	62.156	64.184 ± 1.489	61.909	56.775 ± 1.463	54.591	64.392 ± 1.494	66.510
356	60.434 ± 0.702	58.226	60.936 ± 0.709	59.591	51.530 ± 0.613	49.954	63.682 ± 0.741	65.782
384	57.874 ± 1.751	56.441	57.820 ± 1.664	58.543	46.538 ± 1.430	47.923	64.184 ± 1.874	65.430
511	49.187 ± 0.588	50.379	53.755 ± 0.640	55.032	41.948 ± 0.509	41.357	61.747 ± 0.740	64.136
662	46.681 ± 0.566	46.180	51.104 ± 0.615	52.635	37.125 ± 0.452	37.069	64.507 ± 0.778	63.156
835	43.874 ± 1.191	43.416	53.444 ± 1.523	51.081	35.630 ± 1.040	34.362	60.161 ± 1.745	62.469
1173	40.835 ± 0.502	40.757	48.921 ± 0.599	49.601	30.658 ± 0.376	31.834	62.840 ± 0.773	61.789
1275	39.214 ± 0.451	40.378	51.431 ± 0.592	49.381	32.539 ± 0.375	31.483	58.889 ± 0.679	61.676
1333	41.265 ± 0.462	40.231	51.526 ± 0.578	49.291	32.541 ± 0.367	31.347	64.244 ± 0.719	61.630
Energy (keV)	PbSO <sub>4</sub>		PbCl <sub>2</sub>		PbBr <sub>2</sub>		PbI <sub>2</sub>	
	Exp.	Theo.	Exp.	Theo.	Exp.	Theo.	Exp.	Theo.
81	61.991 ± 0.692	64.947	70.051 ± 0.790	71.786	58.030 ± 0.714	59.817	58.420 ± 0.733	60.746
122	70.103 ± 1.432	71.118	73.324 ± 1.539	76.964	70.141 ± 2.090	73.072	70.074 ± 1.595	70.533
136	67.798 ± 3.017	68.775	72.730 ± 2.791	75.978	70.953 ± 2.802	72.717	67.889 ± 2.688	70.542
161	62.521 ± 1.923	64.676	71.056 ± 1.878	74.125	72.764 ± 2.321	71.923	72.837 ± 2.335	70.453
276	45.620 ± 1.737	47.409	65.343 ± 2.420	64.235	64.444 ± 2.489	66.731	65.955 ± 2.505	69.145
303	43.396 ± 1.019	44.562	60.650 ± 1.463	62.198	67.588 ± 1.608	65.566	70.836 ± 1.689	68.784
356	40.363 ± 0.467	39.980	57.437 ± 0.666	58.604	65.709 ± 0.769	63.451	67.606 ± 0.784	68.084
384	39.691 ± 1.186	38.071	56.612 ± 1.687	56.977	60.863 ± 1.786	62.472	65.842 ± 2.003	67.741
511	31.513 ± 0.374	32.266	52.570 ± 0.631	51.485	57.720 ± 0.691	59.085	64.262 ± 0.768	66.461
662	27.694 ± 0.335	28.768	46.602 ± 0.563	47.705	54.591 ± 0.661	56.672	63.800 ± 0.770	65.466
835	27.288 ± 0.737	26.660	43.334 ± 1.217	45.234	56.981 ± 1.646	55.061	67.049 ± 1.866	64.756
1173	24.120 ± 0.295	24.773	44.381 ± 0.542	42.876	53.211 ± 0.651	53.502	62.127 ± 0.754	64.048
1275	24.029 ± 0.277	24.511	43.778 ± 0.503	42.530	51.226 ± 0.588	53.263	65.825 ± 0.754	63.926
1333	23.618 ± 0.264	24.414	42.925 ± 0.480	42.397	53.892 ± 0.604	53.168	61.756 ± 0.692	63.877

**Table 6**The electron density ( $\times 10^{23}$  electron/g) of the selected samples.

Energy (keV)	BiClO		BiBr <sub>3</sub>		BiF <sub>3</sub>		Bil <sub>3</sub>	
	Exp.	Theo.	Exp.	Theo.	Exp.	Theo.	Exp.	Theo.
81	5.286 ± 0.061	5.152	4.543 ± 0.052	4.665	7.578 ± 0.113	7.647	4.088 ± 0.058	4.235
122	5.554 ± 0.159	5.423	5.743 ± 0.116	5.903	8.336 ± 0.142	8.054	4.810 ± 0.117	4.903
136	5.542 ± 0.243	5.348	6.021 ± 0.286	5.865	7.732 ± 0.383	7.882	4.755 ± 0.221	4.904
161	5.054 ± 0.199	5.209	5.901 ± 0.155	5.783	7.277 ± 0.361	7.570	4.968 ± 0.147	4.897
276	4.381 ± 0.170	4.466	5.175 ± 0.194	5.272	6.214 ± 0.272	6.056	4.772 ± 0.182	4.797
303	4.185 ± 0.099	4.312	5.352 ± 0.124	5.162	5.999 ± 0.155	5.768	4.618 ± 0.107	4.770
356	4.192 ± 0.049	4.039	5.081 ± 0.059	4.969	5.445 ± 0.065	5.278	4.567 ± 0.053	4.718
384	4.015 ± 0.121	3.915	4.821 ± 0.139	4.882	4.917 ± 0.151	5.064	4.603 ± 0.134	4.692
511	3.412 ± 0.041	3.495	4.482 ± 0.053	4.589	4.432 ± 0.054	4.370	4.428 ± 0.053	4.600
662	3.238 ± 0.039	3.204	4.261 ± 0.051	4.389	3.923 ± 0.048	3.917	4.626 ± 0.056	4.529
835	3.044 ± 0.083	3.012	4.456 ± 0.127	4.259	3.765 ± 0.110	3.631	4.315 ± 0.125	4.480
1173	2.833 ± 0.035	2.827	4.079 ± 0.050	4.136	3.239 ± 0.040	3.364	4.507 ± 0.055	4.431
1275	2.720 ± 0.031	2.801	4.289 ± 0.049	4.118	3.438 ± 0.040	3.327	4.223 ± 0.049	4.423
1333	2.863 ± 0.032	2.791	4.296 ± 0.048	4.110	3.438 ± 0.039	3.312	4.607 ± 0.052	4.420
Energy (keV)	PbSO <sub>4</sub>		PbCl <sub>2</sub>		PbBr <sub>2</sub>		PbI <sub>2</sub>	
	Exp.	Theo.	Exp.	Theo.	Exp.	Theo.	Exp.	Theo.
81	8.775 ± 0.098	9.193	5.216 ± 0.059	5.345	3.652 ± 0.045	3.764	3.159 ± 0.040	3.285
122	9.923 ± 0.203	10.067	5.459 ± 0.115	5.730	4.414 ± 0.132	4.598	3.789 ± 0.086	3.814
136	9.597 ± 0.427	9.735	5.415 ± 0.208	5.657	4.465 ± 0.176	4.576	3.671 ± 0.145	3.814
161	8.850 ± 0.272	9.155	5.290 ± 0.140	5.519	4.579 ± 0.146	4.526	3.939 ± 0.126	3.810
276	6.458 ± 0.246	6.711	4.865 ± 0.180	4.783	4.055 ± 0.157	4.199	3.566 ± 0.135	3.739
303	6.143 ± 0.144	6.308	4.516 ± 0.109	4.631	4.253 ± 0.101	4.126	3.830 ± 0.091	3.719
356	5.713 ± 0.066	5.659	4.276 ± 0.050	4.363	4.135 ± 0.048	3.993	3.656 ± 0.042	3.682
384	5.618 ± 0.168	5.389	4.215 ± 0.126	4.242	3.830 ± 0.112	3.931	3.560 ± 0.108	3.663
511	4.461 ± 0.053	4.567	3.914 ± 0.047	3.833	3.632 ± 0.043	3.718	3.475 ± 0.042	3.594
662	3.920 ± 0.047	4.072	3.470 ± 0.042	3.552	3.435 ± 0.042	3.566	3.450 ± 0.042	3.540
835	3.863 ± 0.104	3.774	3.226 ± 0.091	3.368	3.586 ± 0.104	3.465	3.626 ± 0.101	3.502
1173	3.414 ± 0.042	3.507	3.304 ± 0.040	3.192	3.348 ± 0.041	3.367	3.359 ± 0.041	3.463
1275	3.401 ± 0.039	3.469	3.259 ± 0.037	3.167	3.223 ± 0.037	3.352	3.559 ± 0.041	3.457
1333	3.343 ± 0.037	3.456	3.196 ± 0.036	3.157	3.391 ± 0.038	3.346	3.339 ± 0.037	3.454

## Appendix A. Supplementary data

Supplementary data to this article can be found online at <https://doi.org/10.1016/j.net.2018.12.018>.

## References

- [1] H.C. Manjunatha, L. Seenappa, B.M. Chandrika, C. Hanumantharayappa, A study of photon interaction parameters in barium compounds, *Ann. Nucl. Energy* 109 (2017) 310–317.
- [2] D. Han, W. Kim, S. Lee, H. Kim, P. Romero, Assessment of gamma radiation shielding properties of concrete containers containing recycled coarse aggregates, *Constr. Build. Mater.* 163 (2018) 122–138.
- [3] K.J. Singh, N. Singh, R.S. Kaundal, K. Singh, Gamma-ray shielding and structural properties of PbO-SiO<sub>2</sub> glasses, *Nucl. Instrum. Methods B* 266 (2008) 944–948.
- [4] B.O. El-bashir, M.I. Sayyed, M.H.M. Zaid, K.A. Matori, Comprehensive study on physical, elastic and shielding properties of ternary BaO-Bi2O3-P2O5 glasses as a potent radiation shielding material, *J. Non-Cryst. Solids* 468 (2017) 92–99.
- [5] S.S. Obaid, M.I. Sayyed, D.K. Gaikwad, P.P. Pawar, Attenuation coefficients and exposure buildup factor of some rocks for gamma ray shielding applications, *Radiat. Phys. Chem.* 148 (2018) 86–94.
- [6] I. Akkurt, C. Basigit, S. Kilincarslan, B. Mavi, The shielding of  $\gamma$ -rays by concretes produced with barite, *Prog. Nucl. Energy* 46 (2005) 1–11.
- [7] I. Akkurt, H. Akyildirim, B. Mavi, S. Kilincarslan, C. Basigit, Gamma-ray shielding properties of concrete including barite at different energies, *Prog. Nucl. Energy* 52 (7) (2010) 620–623.
- [8] A.S. Ouda, Development of high-performance heavy density concrete using different aggregates for gamma-ray shielding, *Prog. Nucl. Energy* 79 (2015) 48–55.
- [9] M.I. Sayyed, M.G. Dong, H.O. Tekin, G. Lakshminarayana, M.A. Mahdi, Comparative investigations of gamma and neutron radiation shielding parameters for different borate and tellurite glass systems using WinXCom program and MCNPX code, *Mater. Chem. Phys.* 215 (2018) 183–202.
- [10] G. Lakshminarayana, M.I. Sayyed, S.O. Baki, A. Lira, M.G. Dong, K.M. Kaky, et al., Optical absorption and gamma-radiation-shielding parameter studies of Tm<sup>3+</sup>-doped multicomponent borosilicate glasses, *Appl. Phys. A-Mater.* 124 (2018) 378.
- [11] V.P. Singh, N.M. Badiger, N. Chanthima, J. Kaewkhao, Evaluation of gamma-ray exposure buildup factors and neutron shielding for bismuth borosilicate glasses, *Radiat. Phys. Chem.* 98 (2014) 14–21.
- [12] M. Kurudirek, Heavy metal borate glasses: potential use for radiation shielding, *J. Alloy. Comp.* 727 (2017) 1227–1236.
- [13] M.R. Ambika, N. Nagaiah, V. Harish, N.K. Lokanath, M.A. Sridhar, N.M. Renukappa, et al., Preparation and characterisation of Isophthalic-Bi2O3 polymer composite gamma radiation shields, *Radiat. Phys. Chem.* 130 (2017) 351–358.
- [14] V. Harish, N. Nagaiah, T.P. Niranjan, K.T. Varughese, Preparation and characterisation of lead monoxide filled unsaturated polyester based polymer composites for gamma radiation shielding applications, *J. Appl. Polym. Sci.* 112 (2009) 1503–1508.
- [15] V. Harish, N. Nagaiah, H.G.H. Kumar, Lead oxides filled Isophthalic resin polymer composites for gamma radiation shielding applications, *Indian J. Pure Appl. Phys.* 50 (2012) 847–850.
- [16] S. Kumar, B. Lal, P. Aghamkar, M. Husain, Influence of sulfur, selenium and tellurium doping on optical, electrical and structural properties of thin films of lead salts, *J. Alloy. Comp.* 488 (2009) 334–338.
- [17] J.L. Rogers, J.J. Ernat, H. Yung, R.S. Mohan, Environmentally friendly organic synthesis using bismuth compounds. Bismuth (III) bromide catalyzed synthesis of substituted tetrahydroquinoline derivatives, *Catal. Commun.* 10 (5) (2009) 625–626.
- [18] S.S. Obaid, D.K. Gaikwad, P.P. Pawar, Determination of gamma ray shielding parameters of rocks and concrete, *Radiat. Phys. Chem.* 144 (2018) 356–360.
- [19] D.K. Gaikwad, S.S. Obaid, M.I. Sayyed, R.R. Bhosale, V.V. Awasarmol, A. Kumar, et al., Comparative study of gamma ray shielding competence of WO<sub>3</sub>-TeO<sub>2</sub>-PbO glass system to different glasses and concretes, *Mater. Chem. Phys.* 213 (2018) 508–517.
- [20] F. Akman, R. Durak, M.F. Turhan, M.R. Kaçal, Studies on effective atomic numbers, electron densities from mass attenuation coefficients near the K edge in some samarium compounds, *Appl. Radiat. Isot.* 101 (2015) 107–113.
- [21] L. Gerward, N. Guilbert, K.B. Jensen, H. Levring, X-ray absorption in matter: reengineering XCOM, *Radiat. Phys. Chem.* 60 (2001) 23–24.
- [22] F. Akman, İ.H. Geçibesler, M.I. Sayyed, S.A. Tijani, A.R. Tufekci, I. Demirtas, Determination of some useful radiation interaction parameters for waste foods, *Nucl. Eng. Technol.* 50 (2018) 944–949.
- [23] S.S. Obaid, M.I. Sayyed, D.K. Gaikwad, H.O. Tekin, Y. Elmahroug, P.P. Pawar, Photon attenuation coefficients of different rock samples using MCNPX, Geant4 simulation codes and experimental results: a comparison study, *Radiat. Eff. Defect Solid* 7 (2018) 1–15.
- [24] D.K. Gaikwad, P.P. Pawar, T.P. Selvam, Mass attenuation coefficients and effective atomic numbers of biological compounds for gamma ray interactions, *Radiat. Phys. Chem.* 138 (2017) 75–80.
- [25] A. Kumar, Gamma ray shielding properties of PbO-Li<sub>2</sub>O-B<sub>2</sub>O<sub>3</sub> glasses, *Radiat. Phys. Chem.* 136 (2017) 50–53.
- [26] R. Bagheri, A.K. Moghaddam, H. Yousefnia, Gamma ray shielding study of barium-bismuth-borosilicate glasses as transparent shielding materials using MCNP-4C code, XCOM program, and available experimental data, *Nucl. Eng. Technol.* 49 (2017) 216–223.
- [27] F. Akman, R. Durak, M.R. Kaçal, F. Bezgin, Study of absorption parameters around the K edge for selected compounds of Gd, *X Ray Spectrom.* 45 (2) (2016) 103–110.
- [28] F. Akman, M.R. Kaçal, F. Akman, M.S. Soylu, Determination of effective atomic numbers and electron densities from mass attenuation coefficients for some selected complexes containing lanthanides, *Can. J. Phys.* 95 (10) (2017) 1005–1011.
- [29] V.P. Singh, N.M. Badiger, J. Kaewkhao, Radiation shielding competence of silicate and borate heavy metal oxide glasses: comparative study, *J. Non-Cryst. Solid.* 404 (2014) 167–173.
- [30] M.H. Hazlan, M. Jamil, R.M. Ramli, N.Z.N. Azman, X-ray attenuation characterisation of electrospun Bi2O3/PVA and WO<sub>3</sub>/PVA nanofibre mats as potential X-ray shielding materials, *Appl. Phys. A-Mater.* 124 (2018) 497.
- [31] M. Kurudirek, Effective atomic numbers and electron densities of some human tissues and dosimetric materials for mean energies of various radiation sources relevant to radiotherapy and medical applications, *Radiat. Phys. Chem.* 102 (2014) 139–146.
- [32] C.V. More, R.M. Lokhande, P.P. Pawar, Effective atomic number and electron density of amino acids within the energy range of 0.122–1.330 MeV, *Radiat. Phys. Chem.* 125 (2016) 14–20.
- [33] M.I. Sayyed, F. Akman, İ.H. Geçibesler, H.O. Tekin, Measurement of mass attenuation coefficients, effective atomic numbers, and electron densities for different parts of medicinal aromatic plants in low-energy region, *Nucl. Sci. Tech.* 29 (2018) 144.
- [34] M.I. Sayyed, F. Akman, V. Turan, A. Araz, Evaluation of radiation absorption capacity of some soil samples, *Radiochim. Acta* (2018), <https://doi.org/10.1515/ract-2018-2996>.
- [35] F. Akman, İ.H. Geçibesler, İ. Demirkol, A. Çetin, Determination of effective atomic numbers and electron densities for some synthesized triazoles from the measured total mass attenuation coefficients at different energies, *Can. J. Phys.* (2018). <https://doi.org/10.1139/cjp-2017-0923>.